Supplement to: How atmospheric and surface conditions shape recurrent heatwaves in Europe: From local to continental scales

Ines Dillerup[1], Gabriele Messori[2,3,4], Alexander Lemburg[1], Sebastian Buschow[5,6], and Joaquim G. Pinto[1]

[1]Institute for Meteorology and Climate Research - Troposphere Research (IMKTRO), Karlsruhe Institute of Technology (KIT), Karlsruhe, Germany
[2]Department of Earth Sciences, Uppsala University, Uppsala, Sweden
[3]Swedish Centre for Impacts of Climate Extremes (climes), Uppsala University, Uppsala, Sweden
[4]Department of Meteorology, Stockholm University, Stockholm, Sweden
[5]Institute of Geosciences, University of Bonn, Bonn, Germany
[6]Jülich Supercomputing Centre, Forschungszentrum Jülich, Jülich, Germany

Correspondence: Ines Dillerup (ines.dillerup@kit.edu)

Abstract. The supplemental material includes Figure S1-S14 and Tables S1-S3.

S1 Weather Regimes

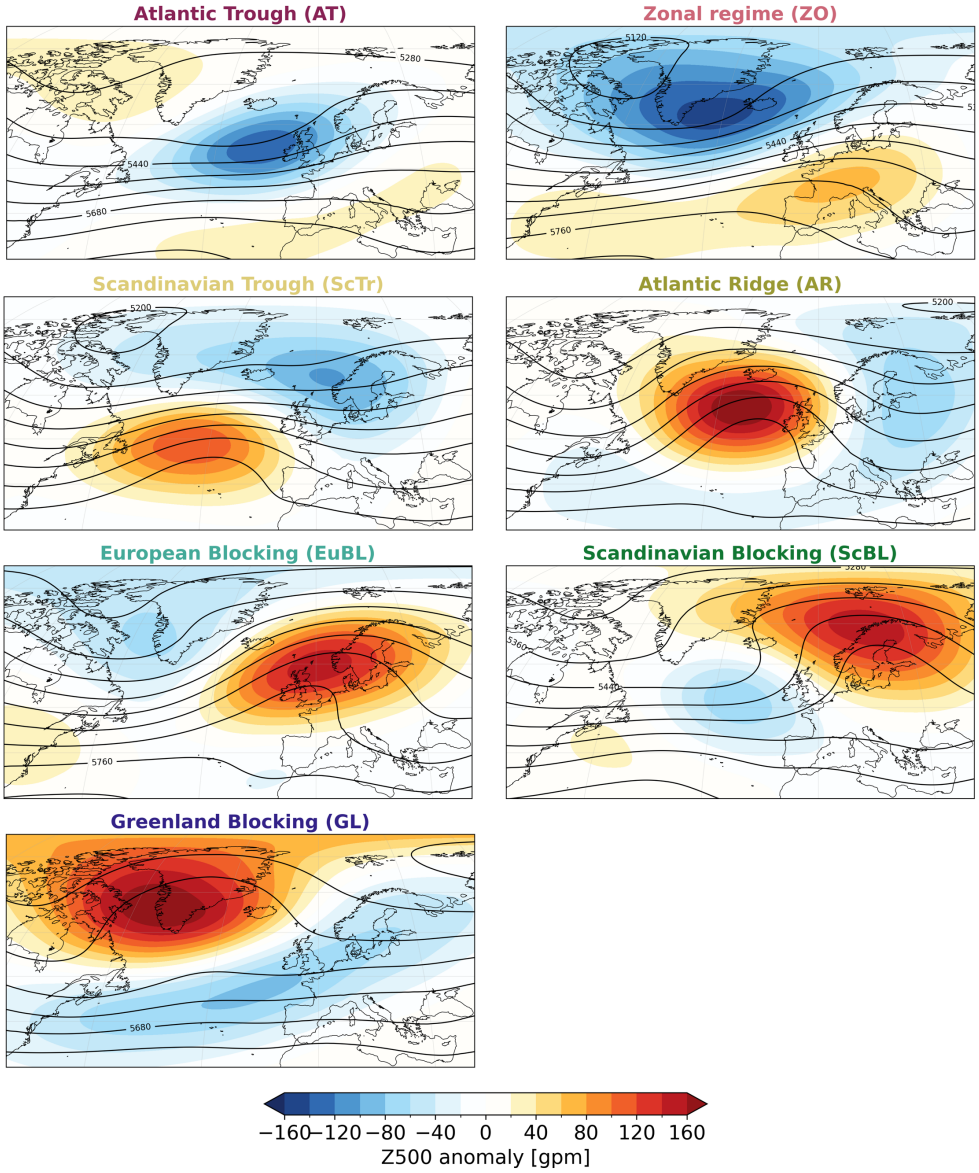

Figure S1. Weather regime cluster means. Mean 500-hPa geopotential height (contours; geopotential meters (gpm)) and corresponding anomalies (shading; gpm) of the seven year-round Atlantic–European weather regimes (Grams, 2026). Figure taken from (Dillerup et al., 2026).

S2 Object recurrence statistics

Table S1. Number of heatwave objects and their durations counted at their onset.

	Heatwave type	May	Jun	Jul	Aug	Sep
duration [d]	strongly recurrent	29.52 ± 30.32	30.06 ± 22.97	40.45 ± 21.19	21.64 ± 12.13	10.75 ± 9.81
(mean $\pm$ std)	weakly recurrent	7.67 ± 4.07	6.92 ± 4.91	11.23 ± 6.10	8.78 ± 6.40	8.62 ± 3.23
number of events	strongly recurrent	21	16	11	11	8
	weakly recurrent	18	12	13	9	13

S3 Sensitivity of Results to the Definition of Recurrence

S3.1 Local Recurrence

To assess the sensitivity of our results to the maximum break duration between two local heatwaves, we repeated the analysis using a maximum break of 3 days following Zhang et al. (2025) and a break of 11 days, corresponding to the same distance from our chosen value of 7 days. The temperature threshold used to define heatwaves is not varied, as both Zhang et al. (2025) and Baldwin et al. (2019) reported that the sensitivity of the results is minor when choosing either the 95th or 90th percentile. Furthermore, following Zhang et al. (2025), we adopt the 90th percentile to ensure a larger sample size for analyzing local recurrent heatwaves.

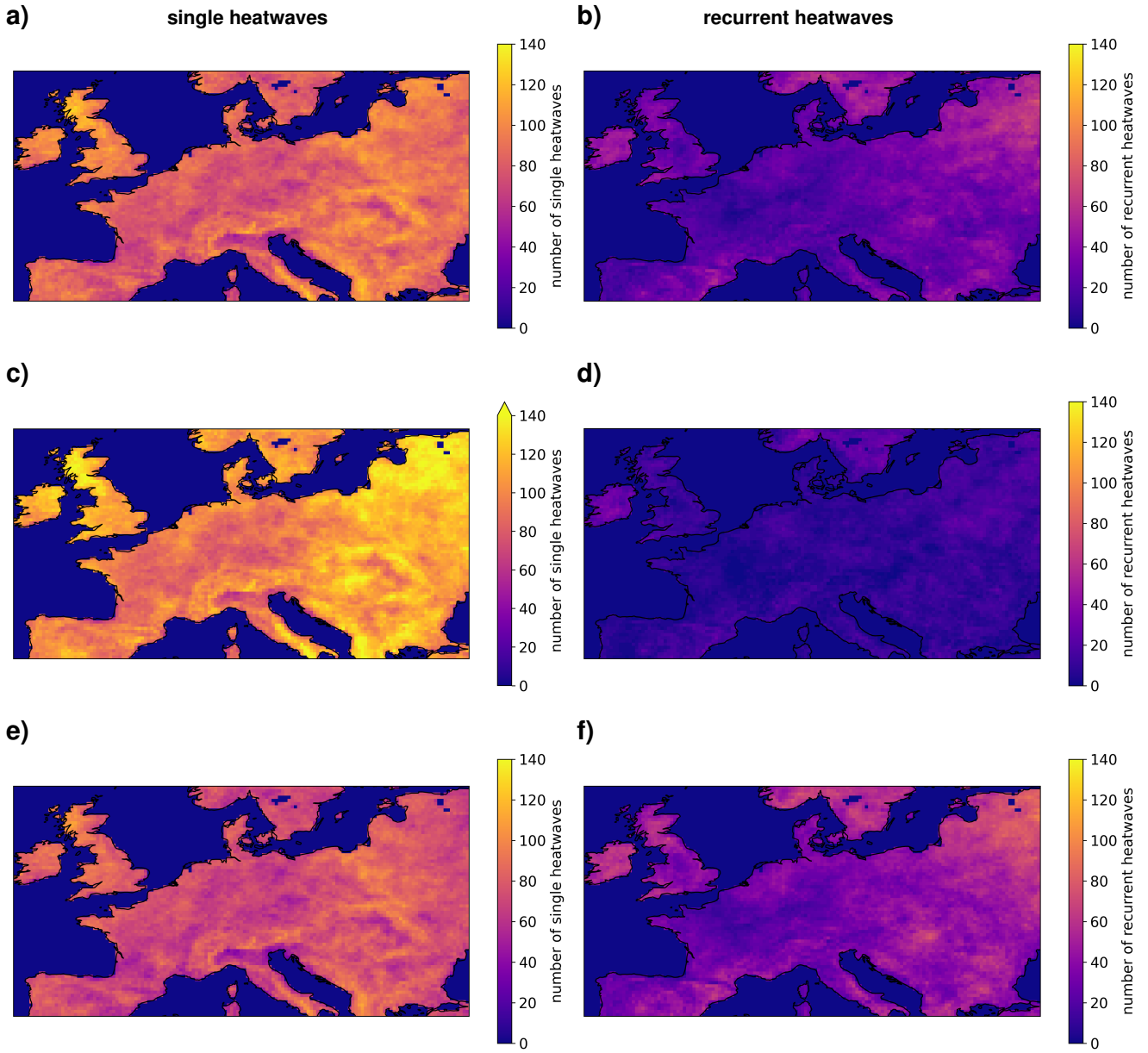

Figure S2. Spatial distribution of single (left) and total recurrent (first+following) (right) heatwaves for maximum break durations: 7d (a,b), 3d (c,d) and 11d (e,f).

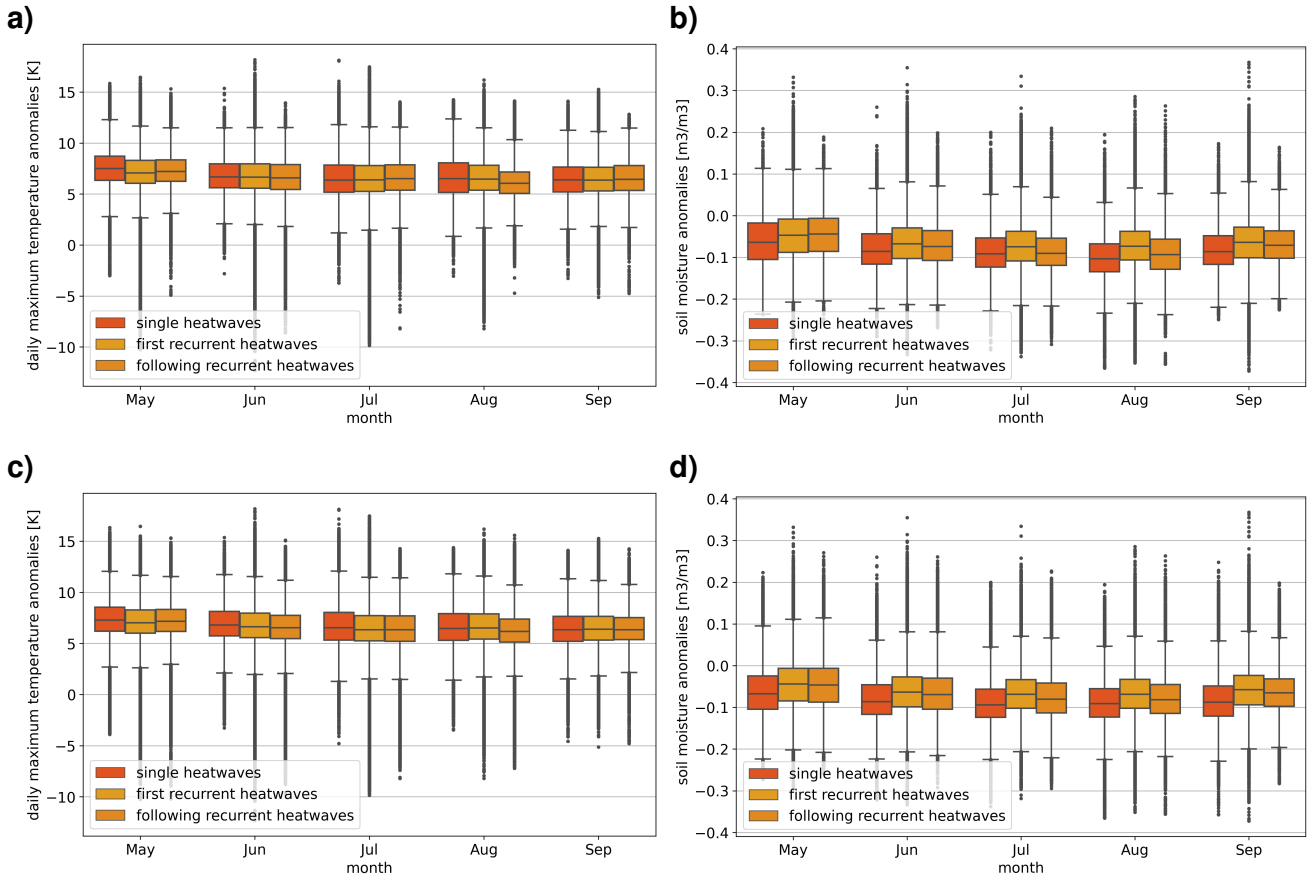

Figure S3. Daily maximum temperature anomalies (a, c) and soil moisture anomalies in the upper layer (b, d) during single and the first and following recurrent local heatwaves stratified per month for a maximum break duration of 3d (a,b) and 11d (c,d). All local heatwaves are assigned to their start month.

Table S2. Monthly durations and proportions of single, first and following recurrent local heatwaves during May to September for maximum break duration 3d (top) and 11d (bottom).

	heatwave type	May	Jun	Jul	Aug	Sep
duration [d]	single	5.64 ± 1.48	5.70 ± 2.31	6.63 ± 3.25	6.47 ± 2.53	4.98 ± 1.55
(mean $\pm$ std)	first	3.33 ± 0.82	6.33 ± 2.59	4.42 ± 1.62	3.41 ± 0.80	3.22 ± 1.84
	following	3.17 ± 0.41	2.95 ± 0.23	6.27 ± 2.79	3.02 ± 0.15	1.4 ± 0.73
proportion	single	91.0	92.1	88.8	90.1	91.6
of events [%]	first	4.9	3.9	5.9	4.5	3.4
	following	4.2	3.9	5.4	5.4	5.0
duration [d]	single	5.54 ± 1.48	5.77 ± 2.13	6.43 ± 2.71	5.32 ± 1.97	4.09 ± 1.07
(mean $\pm$ std)	first	6.72 ± 1.04	7.12 ± 3.14	4.62 ± 1.87	8.70 ± 1.92	2.76 ± 0.79
	following	3.17 ± 0.41	3.90 ± 1.44	6.91 ± 4.18	4.18 ± 2.34	5.82 ± 1.72
proportion	single	65.1	64.4	60.1	62.3	68.9
of events [%]	first	18.7	17.2	17.9	15.7	9.5
	following	16.2	18.3	22.0	22.0	21.5

S3.2 Object Recurrence

Since both object recurrence and continental recurrence rely on the heatwave tracking algorithm, we performed extensive tests to ensure the robustness of our results. We explored different strategies for handling splits and merges, as well as different local recurrence break criteria (3d and 11d maximum). The mean heatwave duration, the area, as well as the number and percentage of the common heat days compared to the results of the main analysis are shown in Table S3. All tests qualitatively confirm the longer duration of strongly recurrent objects and their larger area. However, the heatwave object definition, as well as the definition of local recurrences, changes the relative fraction of local recurrence area compared to total heatwave area, the upper and lower thresholds and therefore the selection of heatwaves. Therefore the number of heat days differ, and their overlap with the main results are only about 40-65 %.

Table S3. Sensitivity analysis for area, duration and number of object heat days for a maximum break in the lcoal recurrences of 3d, and 11d and for an explicit tracking of split and merges. Overlaps are computed relative to the main analysis results (shown results). Percentages are first calculated relative to the shown results, then relative to the respective category. Note that the compared data might have a smaller number of object heat days.

	heatwave recurrence type	shown results	split/merge	3d max break	11d max break
duration [d]	strongly	27.91 ± 23.86	21.04± 15.81	23.87± 18.22	23.06 ± 22.49
(mean ± std)	weakly	8.58 ± 4.98	7.87± 4.66	8.22±6.97	7.50±4.69
area [km2]	strongly	2646715.10	2331496.36	2485200.86	2759925.70
(mean)	weakly	963080.25	851443.63	1107123.56	918170.12
number of	strongly	1544	1197	869	923
object heat days	weakly	520	501	331	313
overlap number	strongly	1544	1017	707	812
of object heat days	weakly	520	296	207	251
overlap of	strongly	100	65.9 / 85.0	45.8 / 81.4	52.6 / 88.0
object heat days [%]	weakly	100	56.9 / 59.1	39.8 / 62.5	48.3 / 80.2

Nevertheless, the higher daily maximum temperature anomalies and soil moisture anomalies in the upper layer around the heatwave centroids are robust (Figure S4 and S5), as well as the spatial distribution of the hotspots. Differences arise in the relative and absolute frequencies of some weather regimes.

In addition, the results for object recurrence for the approach in which, during a split or merge event, the heatwave ID of the largest object is retained, are shown here. However, this method introduces ambiguities, as a single local heatwave may be associated with multiple object IDs over time. As the object recurrence analysis is restricted to recurrences within a single object, this complicates a consistent interpretation. For the following results, the ID during the start of the local heatwave was assigned to the local heatwave.

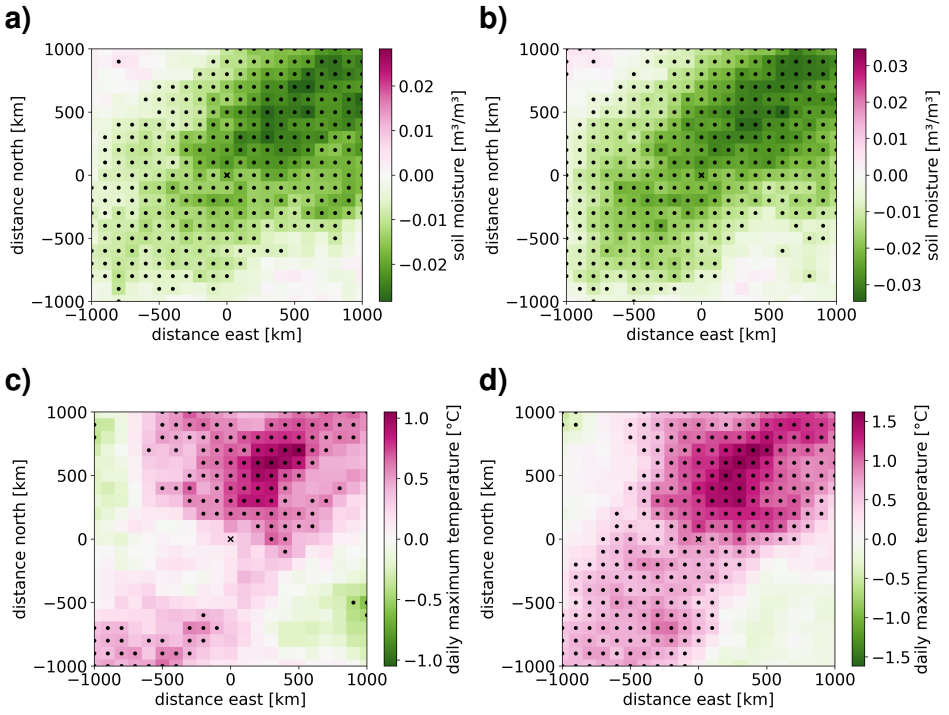

Figure S4. Centered composites difference between strongly and weakly recurrent heatwave objects for soil moisture anomalies (a,b) and daily maximum temperature anomalies (c,d) for 3 day (a,c) and 11 day maximum break (b,d) for the local recurrences. Data is averaged for all heatwaves, with the composites centered on the heatwave centroid and the data composited relative to the distance to it. Dots represent statistically significant differences between strongly and weakly recurrent heatwaves based on a t-test at the 5% significance level following an FDR correction.

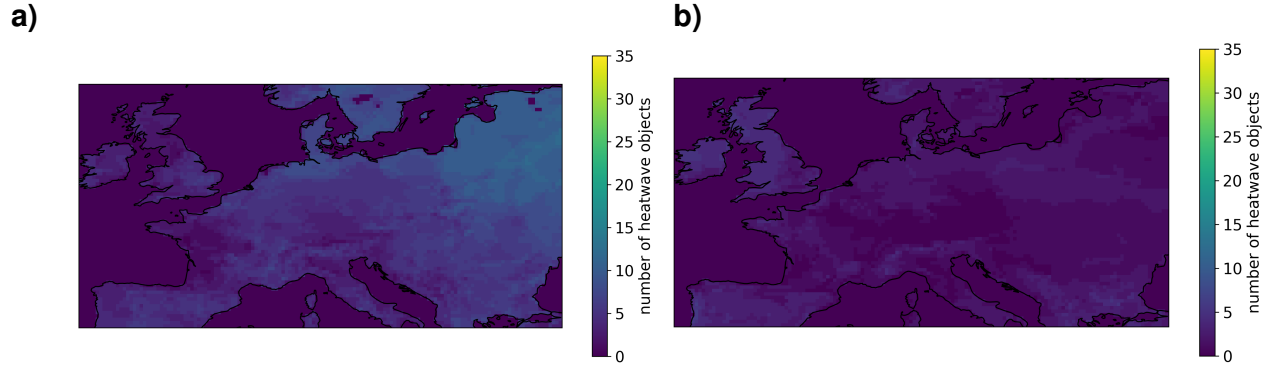

Figure S5. Spatial distribution of strongly (a) and weakly (b) recurrent heatwaves for explicit tracking of splits and merges. Shown is the total number of different heatwave objects per grid cell.

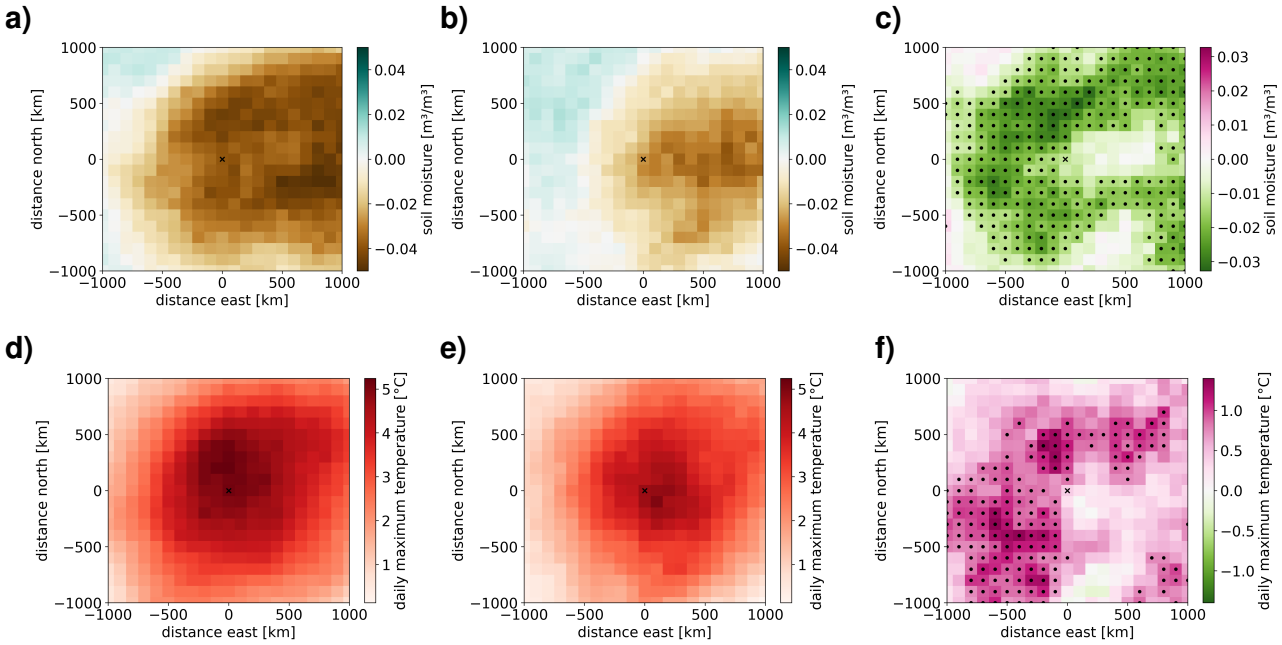

Figure S6. Centered composites showing the difference (right) between strongly (left) and weakly (middle) recurrent heatwaves in soil moisture anomalies in the upper soil layer (a-c) and detrended daily maximum temperature anomalies (d-f) for explicit split and merge tracking. Data is averaged for all heatwaves, with the heatwave centroid in the center and the data aligned and averaged relative to the distance to it. Dots represent statistically significant differences between strongly and weakly recurrent heatwaves based on a t-test and FDR correction.

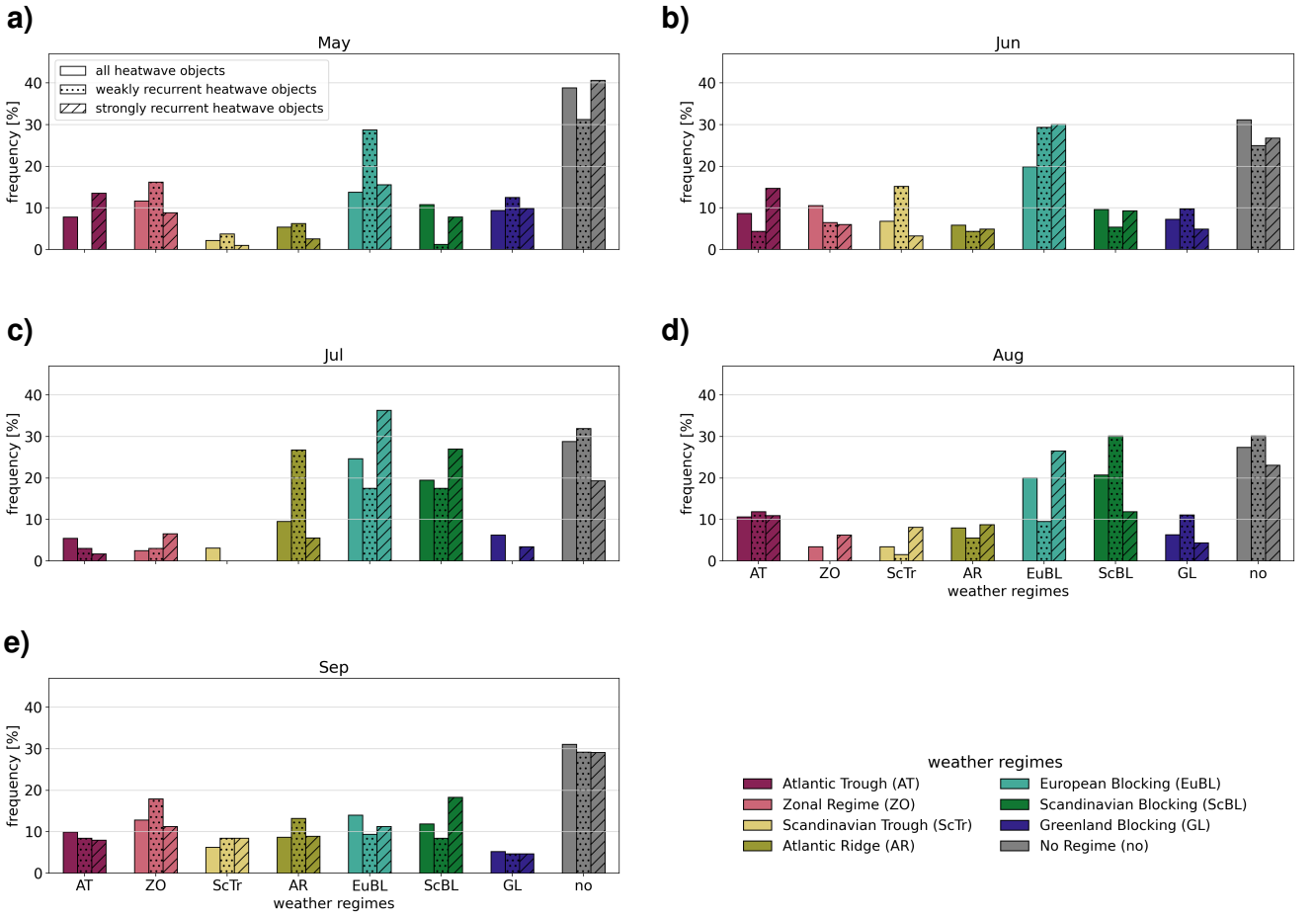

Figure S7. Monthly weather regime frequencies for all, weakly recurrent, and strongly recurrent heatwaves for explicit split and merge tracking. No hatching: all heatwaves; dotted: weakly recurrent; striped: strongly recurrent. The spatial weather regime clusters are illustrated in Appendix S1.

S3.3 Continental Recurrence

Because continental recurrence depends on the heatwave tracking algorithm, we performed extensive tests to assess the robustness of our results. Key parameters, including overlap and clustering distance, were systematically varied, and alternative strategies for handling splits and merges were explored. We also varied the minimum threshold for the number of heatwaves per grid cell and compared results based on the area × number of heatwaves criterion with those using area alone. The selected strongly and weakly recurrent summers are shown in Figure S8, while Table S9 summarizes the number of matching years in each category and the changes in yearly classification. Differences, when they occur, involve transitions between neutral and strongly/weakly recurrent categories, whereas direct changes between strongly and weakly recurrent summers are generally

absent, except under the most restrictive criterion of more than four heatwaves. The classification of most years is largely unchanged across all tested scenarios. This demonstrates the robustness of our classification.

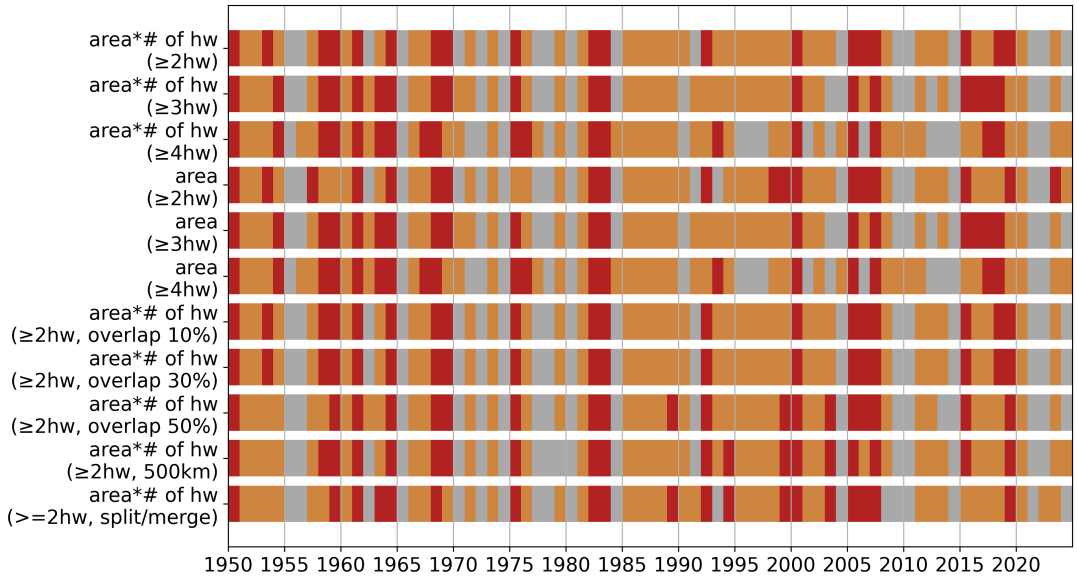

Figure S8. Classification of strongly and weakly recurrent summers for different heatwave number thresholds, overlaps, centroid distance, split/merge handling and detection methods based on area times number of heatwaves or solely on the area.

	wr->wr	wr->n	n->wr	n->n	n->sr	sr->n	sr->sr	sr->wr	wr->sr
area*# of hw (>=2hw)	19	0	0	37	0	0	19	0	0
area*# of hw (>=3hw)	16	3	3	30	4	4	15	0	0
area*# of hw (>=4hw)	9	10	9	22	6	5	13	1	0
area (>=2hw)	18	1	1	32	4	4	15	0	0
area (>=3hw)	16	3	3	30	4	4	15	0	0
area (>=4hw)	9	10	9	22	6	5	13	1	0
area*#of hw (>=2hw, overlap 10%)	19	0	0	37	0	0	19	0	0
area*# of hw (>=2hw, overlap 30%)	19	0	0	37	0	0	19	0	0
area*# of hw (≥2hw, overlap 50%)	18	1	1	33	3	3	16	0	0
area*# of hw (≥2hw, 500km)	18	1	1	33	3	3	16	0	0
area*# of hw (>=2hw, split/merge)	17	2	2	30	5	5	14	0	0

wr = weakly recurrent | n = neutral | sr = strongly recurrent

Figure S9. Transition table showing the category changes relative to the implemented (area*of hw (>=2hw)) .

Moreover, the results for continental recurrence for the approach in which, during a split or merge event, the heatwave ID of the largest object is retained, are shown in the following. All main conclusions remain robust.

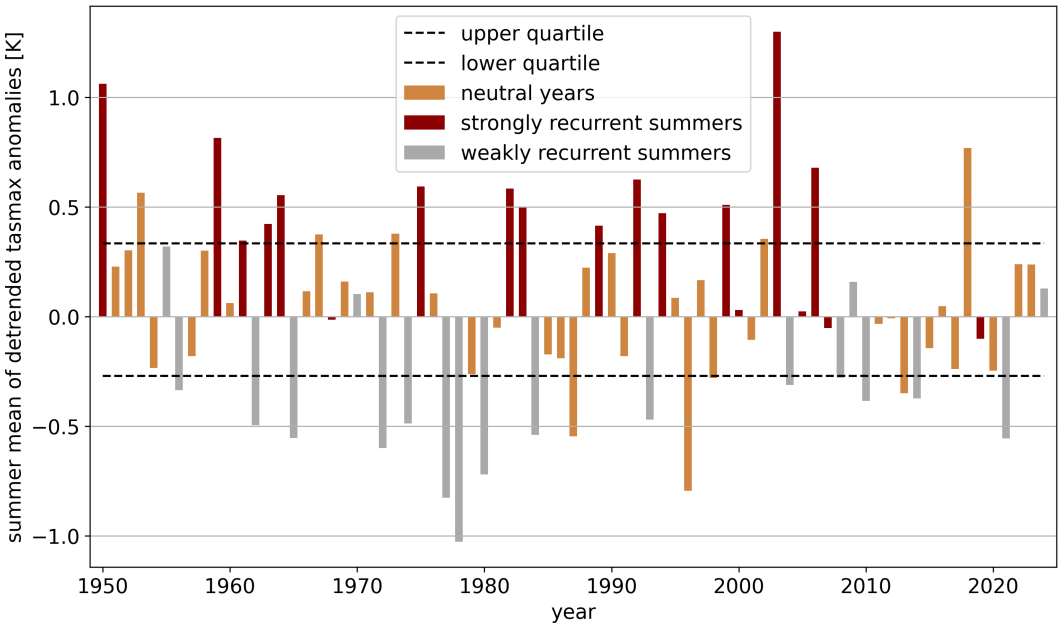

Figure S10. Yearly daily maximum temperature anomalies in the extended summer months colored in the seasonal recurrence classification for explicit split and merge tracking. Red indicates strongly recurrent summers, grey weakly recurrent summers, and orange years which lie in between. The dashed lines represent the upper and lower quartiles of detrended daily maximum temperature anomalies, as an indication of hot and cold years.

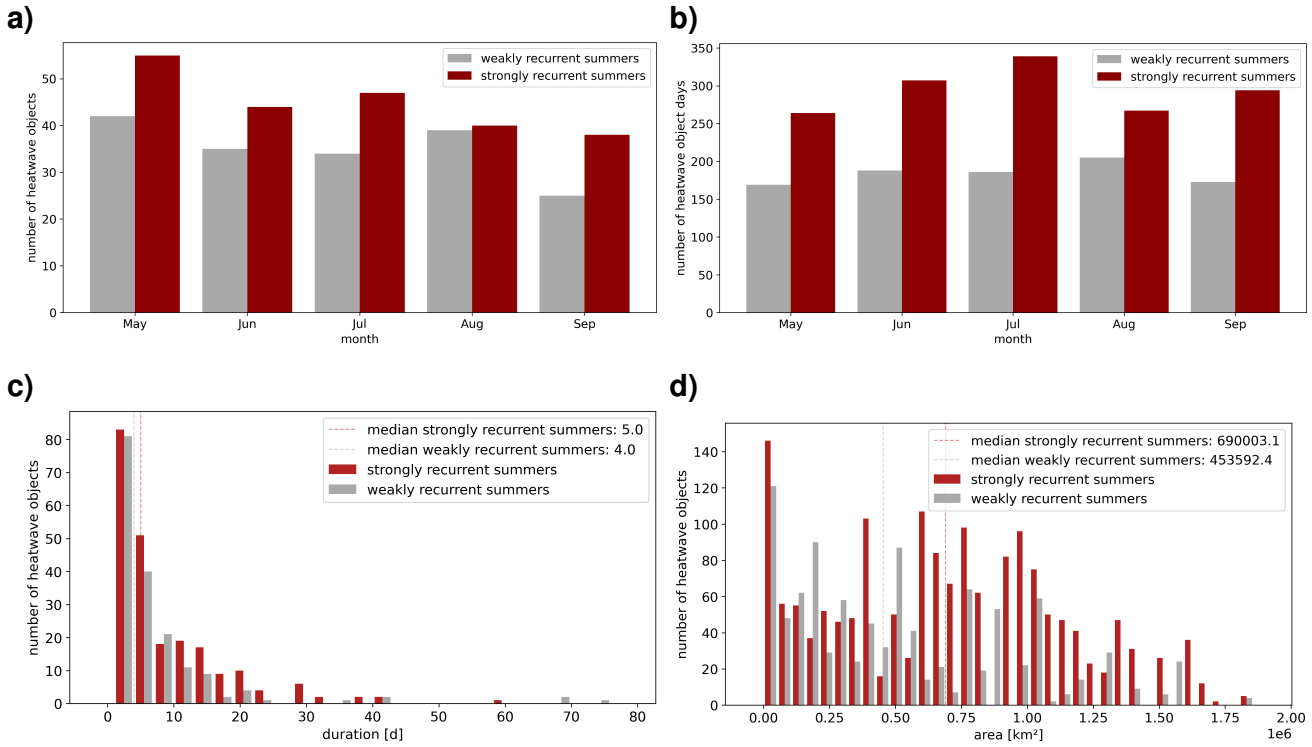

Figure S11. Basic statistics for strongly and weakly recurrent summers for explicit split and merge tracking. (a) monthly number of heatwaves (with each heatwave assigned to the month with the higher number of heat days, if equal to the start month), (b) monthly number of object heat days, (c) duration and (d) area histogram of heatwave objects for all months with dashed lines indicating the median for both year types.

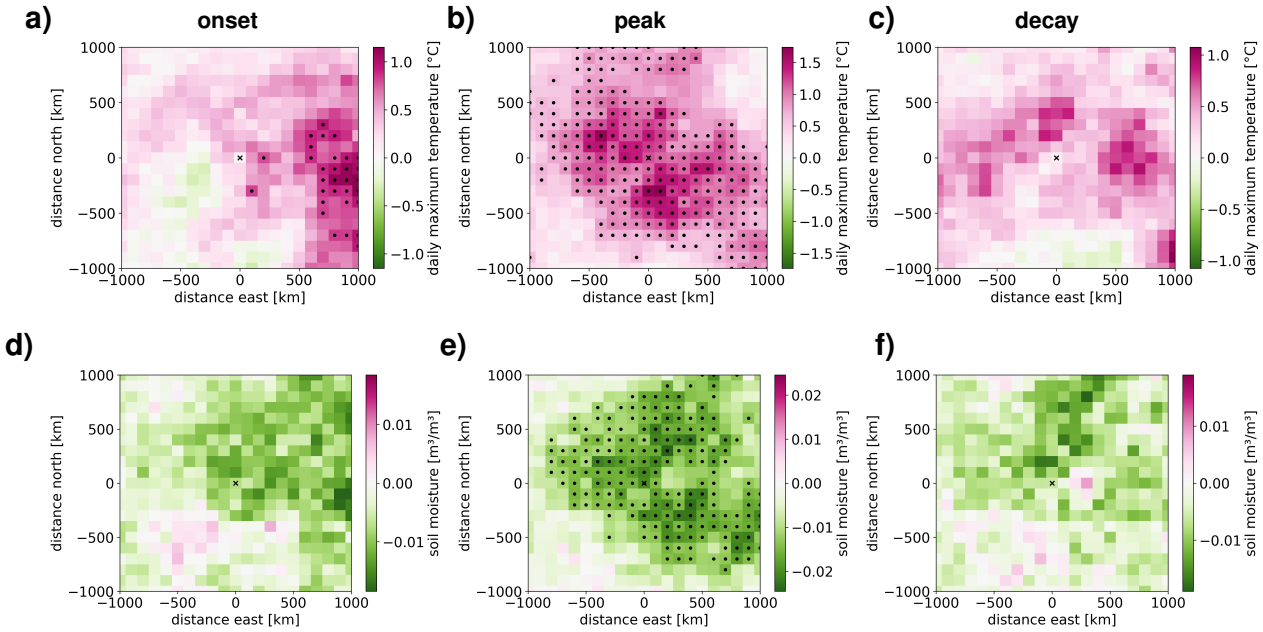

Figure S12. Centered composites showing the difference between strongly and weakly recurrent summers in detrended daily maximum temperature anomalies (a-c) and soil moisture anomalies in the upper soil layer (d-f) for the heatwave onset (left), peak (middle), and decay (right) for explicit split and merge tracking. Data is averaged for all heatwaves, with the composites centred on the heatwave centroid and the data composited relative to the distance to it. Dots represent statistically significant differences between strongly and weakly recurrent summers based on a t-test at the 5% significance level following an FDR correction.

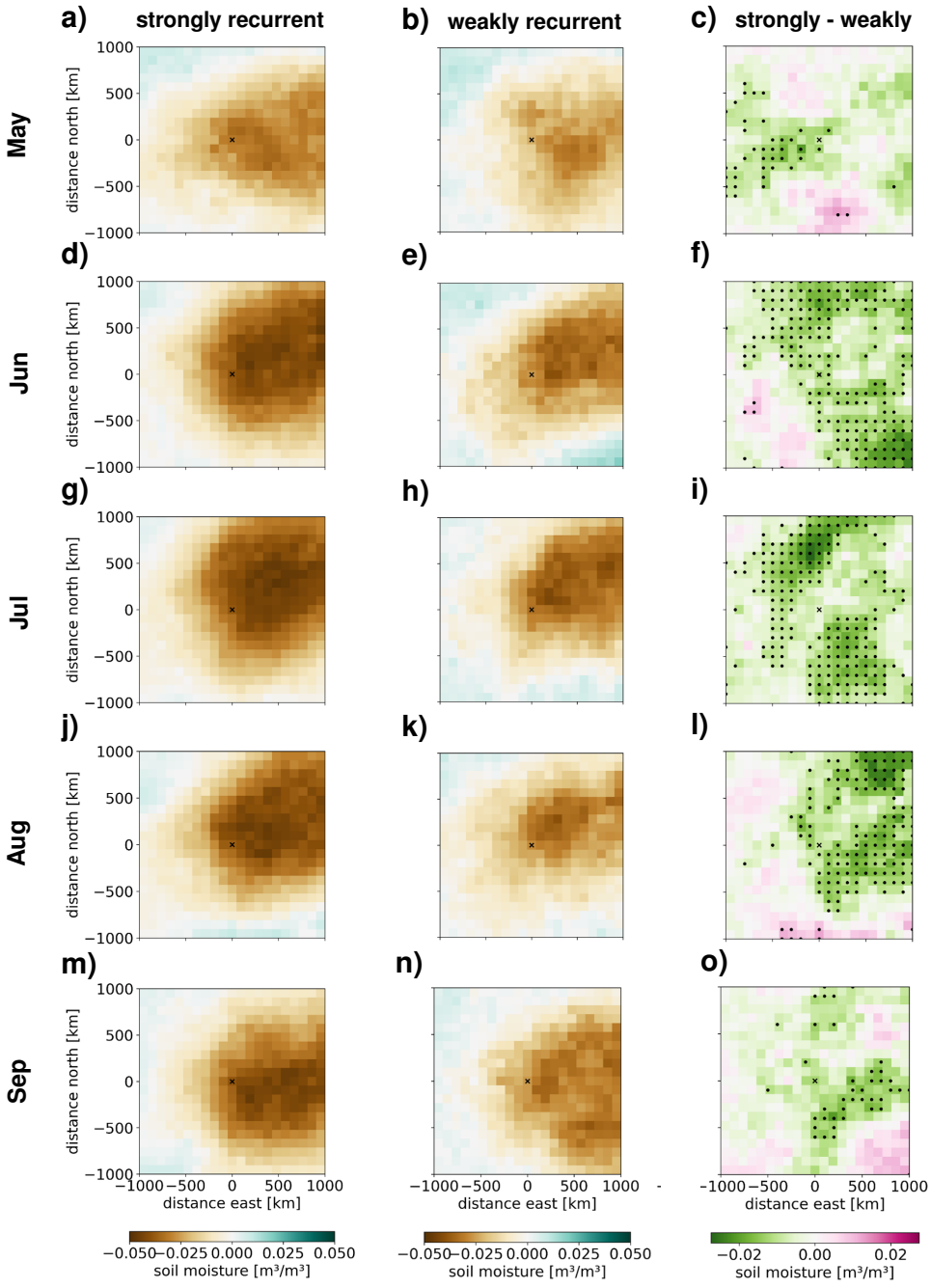

Figure S13. Centered composites showing soil moisture anomalies in the upper soil layer relative to the heatwave centroid split into the months May to September (rows) for explicit split and merge tracking. The left column corresponds to heatwaves in strongly compound summers, the middle column to heatwaves in weakly compound summers and the right column to the difference between them. Data is averaged for all heatwaves, with the heatwave centroid in the center and the data aligned and averaged relative to the distance to it. Dots represent statistically significant differences between strongly and weakly recurrent summers based on a t-test and FDR correction.

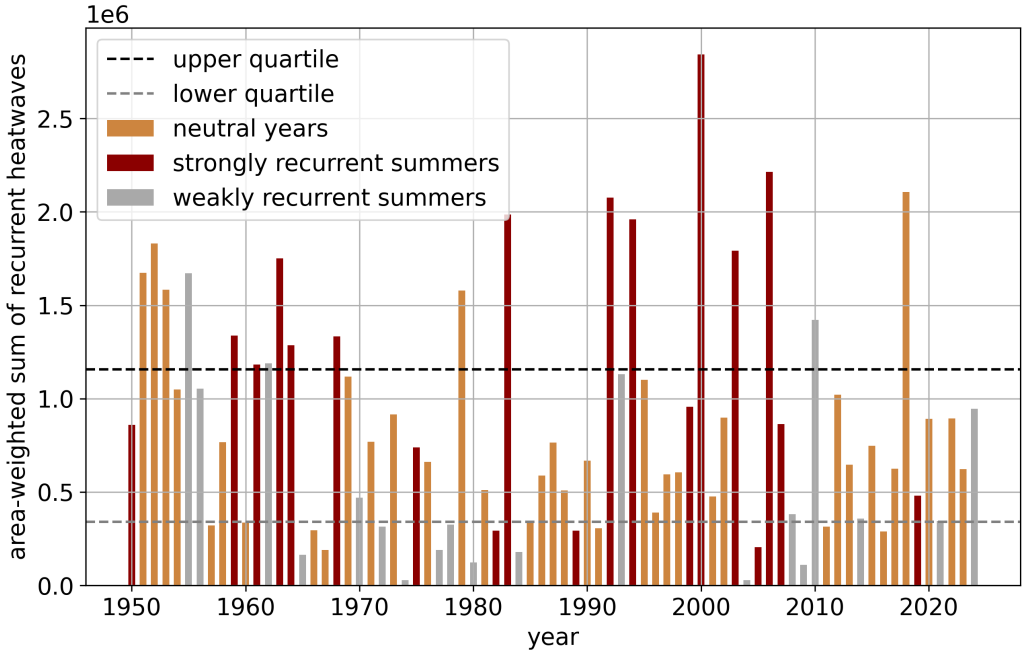

Figure S14. Area-weighted sum of number of local recurrences per year for explicit split and merge tracking. Red colors indicate strongly recurrent summers, grey weakly recurrent summers, and orange neutral summers. Dashed lines indicate the 25th and 75th percentiles of the local recurrence sum.

References

Baldwin, J. W., Dessy, J. B., Vecchi, G. A., and Oppenheimer, M.: Temporally Compound Heat Wave Events and Global Warming: An Emerging Hazard, Earth's Future, 7, 411–427, https://doi.org/10.1029/2018EF000989, 2019.

Dillerup, I., Lemburg, A., Buschow, S., and Pinto, J. G.: Dynamical system metrics and weather regimes explain the seasonally-varying link between European heatwaves and the large-scale atmospheric circulation, Earth System Dynamics, 17, 265–289, https://doi.org/10.5194/esd-17-265-2026, 2026.

Grams, C. M.: A life cycle definition of year-round weather regimes in the North Atlantic European region, EGUsphere [preprint], 2026, 1–60, https://doi.org/10.5194/egusphere-2025-6385, 2026.

Zhang, L., Liao, W., Chen, X., Cheng, S., and Yang, J.: Temporally Compound Heatwave and Its Interaction With Urban Heat Island Over Mainland China, Earth's Future, 13, e2025EF006 490, https://doi.org/10.1029/2025EF006490, 2025.